*horticulturae*

MDPI

*Article*

# Evaluation of In Vitro and In Vivo Antifungal Activity of Green Synthesized Silver Nanoparticles against Early Blight in Tomato

**Madeeha Ansari [1,*], Shakil Ahmed [1], Muhammad Tajammal Khan [1,2], Najwa A. Hamad [3], Hayssam M. Ali [4], Asim Abbasi [5,*], Iqra Mubeen [6], Anum Intisar [7,8], Mohamed E. Hasan [9] and Ihsan K. Jasim [10]**

1 Institute of Botany, University of the Punjab, Lahore 54590, Pakistan
2 Department of Botany, Division of Science and Technology, University of Education, Lahore 54770, Pakistan
3 Plant Protection Department, Faculty of Agriculture, Omar Al-Mukhtar University, El-Beida P.O. Box 919, Libya
4 Department of Botany and Microbiology, College of Science, King Saud University, Riyadh 11451, Saudi Arabia
5 Department of Environmental Sciences, Kohsar University Murree, Punjab 47150, Pakistan
6 State Key Laboratory of Rice Biology, Institute of Biotechnology, Zhejiang University, Hangzhou 310058, China; iqra.kynat1@gmail.com
7 Department of Plant Pathology, College of Agriculture, University of Sargodha, Sargodha 40100, Pakistan
8 Department of Plant Pathology and Microbiology, Iowa State University, Ames, IA 50011, USA
9 Bioinformatics Department, Genetic Engineering and Biotechnology Research Institute, University of Sadat City, Sadat City 32897, Egypt
10 Department of Pharmacology, Al-Turath University College, Baghdad 10013, Iraq
* Correspondence: madeeha.phd.botany@pu.edu.pk (M.A.); asimuaf95@gmail.com (A.A.)

**Abstract:** Silver nanoparticles have gained considerable interest in recent decades due to their antimicrobial activity and are used in water disinfection, wound healing, food packaging, and plant protection. This study tested the potential of silver nanoparticles synthesized using the neem (*Azadirachta indica*) leaf extract against *Alternaria solani* causes early blight disease in tomato plants. The pathogen was isolated from infected tomato plants and identified using morphological and molecular features. The results showed significant variation among isolates. Isolates, Shk-1 and Ksr-1 were highly pathogenic, causing up to 80% disease incidence. The potential of silver nanoparticles against each isolate was determined using different concentrations of silver nanoparticles. During in vitro and in vivo experiments, the growth inhibition rate of the pathogen was 70–100% at 50 ppm. Lower concentrations of silver nanoparticles (5 and 10 ppm) increased phenolics, PO, PPO, and PAL production by more than 50% as compared to the untreated control. These defensive mechanisms clearly demonstrate the fungicidal potential of AgNPs and recommend their utilization in different crop protection programs.

**Keywords:** silver nanoparticles; green synthesis; antifungal activity; *Alternaria solani*; tomato; early blight disease



**Citation:** Ansari, M.; Ahmed, S.; Khan, M.T.; Hamad, N.A.; Ali, H.M.; Abbasi, A.; Mubeen, I.; Intisar, A.; Hasan, M.E.; Jasim, I.K. Evaluation of In Vitro and In Vivo Antifungal Activity of Green Synthesized Silver Nanoparticles against Early Blight in Tomato. *Horticulturae* **2023**, *9*, 369. https://doi.org/10.3390/horticulturae9030369

Academic Editors: Loredana Sigillo and Eliana Dell'olmo

Received: 25 January 2023
Revised: 9 March 2023
Accepted: 9 March 2023
Published: 12 March 2023



## 1. Introduction

Nanotechnology has received much attention due to its applications in many industries, such as medical imaging, therapy, drug delivery, and energy generation [1]. Nanotechnology is a field of science and technology that focuses on the study, design, creation, manipulation, and use of materials and devices on the nanoscale level [2]. A nanometer is one billionth of a meter, which means that nanotechnology deals with materials and devices that are typically between 1 and 100 nanometers in size [3]. Due to their smaller size, nanoparticles have a higher surface-to-volume ratio, making them more effective with different properties than their bulk material [4]. Nanotechnology has broad applications in many fields, including electronics, energy, medicine, and agriculture [5].

Applications of nanomaterials, primarily biological applications, depend on their synthesis methods. Nanoparticles are generally synthesized using different physical or chemical approaches [6,7]. However, physical processes usually involve the maintenance of high temperatures and pressures and require more energy, due to which the quality of the product is also compromised. Moreover, chemical methods utilize hazardous synthetic chemicals that persist in the environment and cause pollution [8,9]. Therefore, green synthesis is more of a focus now because using plants to synthesize nanoparticles is a simple, single-step, fast, economic, and eco-friendly approach [10,11]. Green nanoparticle synthesis refers to synthesizing nanoparticles using natural materials such as plants and avoiding harmful chemicals and high temperatures [12]. Green synthesis methods synthesize biocompatible and biodegradable nanoparticles, making them suitable for agricultural applications [13,14]. Plants produce biomolecules like carbohydrates, proteins, polyphenols, and co-enzymes that can reduce silver to silver nanoparticles [15,16].

Silver nanoparticles are the most promising among all the metallic nanoparticles due to their unique properties, physiochemical activities, and potential biological applications [13], including antimicrobial [17], anti-inflammatory, anti-infectious, and antiseptic properties, even at lower concentrations [18]. AgNPs are used as drug delivery agents, cancer therapeutics, and wound healing agents. AgNPs have been investigated for their potential use in environmental remediation, such as water purification and air filtration [19]. AgNPs are being studied for their potential applications in electronics, particularly in developing electronic devices, due to their high electrical conductivity and thermal stability [20]. Moreover, AgNPs have also shown promising results in agriculture for their potential use as an alternative to chemical fertilizers and pesticides [21]. AgNPs improve crop yield and enhance plant growth [22]. AgNPs have also been found to possess antifungal and antibacterial properties, making them suitable for controlling different plant diseases [23].

Silver nanoparticles release silver ions, disrupting the cell membrane and inhibiting the growth of bacteria, fungi, and viruses. The small size of silver nanoparticles allows for high surface area-to-volume ratios and releases more silver ions to counter microbial activity [24]. This property makes silver nanoparticles a promising alternative to traditional antibiotics for treating infectious diseases and a potential ingredient in antimicrobial coatings, textiles, and medical devices [1,18]. It is observed that silver nanoparticles do not affect living cells at lower concentrations, so they cannot provoke microbial resistance [25]. Silver nanoparticles have a high surface area to volume ratio, which allows them to interact with a large number of microbial cells at once. Silver nanoparticles penetrate the cell wall of the microbe and interact with the cell membrane, leading to disruption of the membrane [14]. Silver nanoparticles generate reactive oxygen species (ROS) that damage cellular components, such as DNA and proteins. The mechanism of action is particularly effective against bacteria and fungi, which have a simpler defense system against ROS compared to higher organisms [26]. Silver nanoparticles also interfere with cell signaling pathways, preventing them from communicating with each other and coordinating their response to stressors, which ultimately results in their inability to adapt to changing environments [24]. Silver nanoparticles have a broad spectrum of activity against many different types of microorganisms, which makes it less likely for any one microbe to develop resistance to it [27]. Even if a few microbes do develop resistance, the diverse mechanisms of action of silver nanoparticles make it difficult for them to spread their resistance to other microbes [28].

Many researchers have reported the antimicrobial potential of silver nanoparticles against various pathogens [29–31], including *Alternaria*, *Corynespora*, and *Fusarium* spp. [32]. Genus *Alternaria* Nees is a broad fungal group. Its species, especially *solani* Sorauer, is the most destructive one that causes an Early Blight disease in tomato and potato plants worldwide [33,34]. *Alternaria solani* colonizes the leaves, stems, and fruits [35,36] of plants belonging to the family Solanaceae, causing up to 78% of crop losses [37]. The genetic variation in *A. solani* results in morphological, physiological, and pathogenesis differences among isolates [38]. Many practices have been introduced, such as crop rotation, resistant

cultivars, sanitation, and synthetic fungicides to manage Early Blight disease, but have failed [39,40]. Silver nanoparticles can be used due to their antimicrobial potential; however, there are concerns about their potential toxicity and environmental impacts. Nanoparticles usually cause irreversible damage to living cells by oxidative stress, which solely depends on the size, composition, and concentration of the NPs. Hence, research regarding the identification of optimal doses of NPs against plant diseases is needed [4].

The present study aimed to evaluate the in vitro and in vivo antifungal activity of green synthesized silver nanoparticles (AgNPs) against *Alternaria solani*. The identification and occurrence of *A. solani* were also investigated to understand the distribution and prevalence of the pathogen in tomato crops, which is critical for disease management strategies. In addition, the characteristics of the AgNPs using various analytical techniques were also studied.

## 2. Materials and Methods

### 2.1. Materials

Leaves of the *Azadirachta indica* A. Juss. (neem) plant were collected from the ground (31.497185°-N, 74.298172°-E) of University of the Punjab (Lahore, Pakistan), washed, and dried for further use. Seeds of tomato (*Solanum lycopersicum* L.) varieties were obtained from the Vegetable Research Institute of Ayyub Agricultural Research Institute (AARI), Faisalabad, Pakistan. The required chemicals, i.e., silver nitrate ($AgNO_3$), potato dextrose agar (PDA), methanol, Folin–Ciocalteu reagent, sodium carbonate, Catechol, phosphate buffer, Guaiacol, hydrogen peroxide, sodium phosphate, trichloroacetic acid, and L-phenylalanine were bought from Sigma-Aldrich, United States through Science Traders.

### 2.2. Green Synthesis of Silver Nanoparticles

The silver nanoparticles were synthesized using leaves extract of neem plant prepared in distilled water. The dried leaves of the neem plant were ground using an electric grinder to make fine powder material. Ten (10) grams of the powder material was added to 100 mL of distilled water, boiled for 30 min, cooled at room temperature, and filtered using Whatman's No. 1 filter paper. The plant extract of 20 mL was then reacted with 10 mL of 1 mM silver nitrate solution and incubated for 3 h at 70 °C. The production of AgNPs synthesis was confirmed by observing the solution's color change. Then, the resulting solutions were subjected to UV–vis spectroscopy within 300–800 nm wavelength. Each solution was taken in Eppendorf's tube and centrifuged. The pellet was again centrifuged after dissolving in distilled water. The cycle of centrifugation was repeated several times until purified AgNPs were acquired. The synthesized silver nanoparticles were stored at 4 °C to study their characteristic features.

### 2.3. Characterization of Silver Nanoparticles

Green synthesized silver nanoparticles using leaf extract of *A. indica* (neem) plant were subjected to various techniques, i.e., UV–spectrophotometry, Fourier-transform infrared spectroscopy (FTIR) analysis, zeta sizer, X-ray diffraction (XRD), and scanning electron microscopy (SEM) to determine their size, surface structure, morphology, and other characteristics.

#### 2.3.1. UV–Spectrophotometry of AgNPs

This technique was used to confirm the synthesis of silver nanoparticles. The 1 mL of the sample was taken in Eppendorf's tube and centrifuged at 14,000 rpm for 10 min. After discarding the supernatant, the pellet was dissolved in distilled water again. The procedure was repeated three times to get rid of debris. The purified silver nanoparticles were dissolved in 1 mL of distilled water using a vortex meter and subjected to UV–vis analysis. The absorption spectrum within the 300–800 nm wavelength range on a UV–visible spectrophotometer was taken.

#### 2.3.2. Fourier-Transform Infrared Spectroscopy (FTIR) Analysis of AgNPs

Fourier transform infrared spectroscopy (FTIR) was calibrated to study the organic functional groups attached to the surface of AgNPs. The selected nanoparticles, synthesized at optimized conditions, were purified using repeated centrifugation at 14,000 rpm for 10 min and dried at 60 °C. The dried samples were mixed with a fine powder of potassium bromide (Kbr) and analyzed by FTIR.

#### 2.3.3. X-ray Diffraction (XRD) Analysis of AgNPs

X-ray diffraction (XRD) was used to examine the overall oxidation state and crystal structure of AgNPs. Synthesized nanoparticles were purified by centrifugation, and the resulting pellets were dispersed into 10 mL of deionized water. After freeze-drying the purified AgNPs, the structure was analyzed with XRD.

#### 2.3.4. Scanning Electron Microscopy (SEM) of AgNPs

Scanning electron microscopy (SEM) was performed to envision the morphology of synthesized particles at the submicron scale and elemental information at the micron scale. It provided the exact magnitude and figure of AgNPs. Thin films of the sample were prepared on a carbon-coated copper grid. A drop of AgNPs was placed on carbon-coated copper grids and allowed to stand for two min, and the excess solution was removed using a blotting paper. Then, the film on the grid was allowed to dry at room temperature and exposed to an electron beam.

### *2.4. Isolation of Pathogen*

Pathogen (*Alternaria solani*) was isolated from infected leaves of the diseased tomato plants grown in tunnels and fields of Lahore, Kasur, Faisalabad, Bahawalpur, and Multan. The leaves showing distinctive symptoms of early blight disease were collected in sterilized polythene bags, labeled, and brought to the laboratory for further procedure. The infected parts of leaves were cut into 1–2 cm pieces and placed in one of the surface disinfectant solutions (1% sodium hypochlorite) for 30 s, washed with distilled water, and blotted. These surface-sterilized pieces were placed on PDA media, three to five per Petri plate, with sterilized forceps. The Petri plates were incubated at 27 ± 2 °C for 7 days, and fungal isolates were sub-cultured for purification and identification [41]. Freshly prepared Petri plates were used to purify the pathogen culture from the original culture plate using single spore culture method. A single fungal colony that appeared on the original plate free from contamination was selected to transfer the fungal spore with a sterile inoculation loop. The fresh cultural plates were incubated at 27 ± 2 °C for future use.

### *2.5. Identification of Pathogen*

The isolated fungal pathogen was identified using morphological characteristics, i.e., color, zonation, margin, and diameter of the colony. The size and shape of conidia were observed microscopically at 10×, 40×, and 100× [42], and photographs were taken to compare with the literature [43–45]. Molecular identification was performed by extracting DNA using the 2% CTAB method [46]. The primer pair ITS1 (5-TCCGTAGGTGAACCTGCGG-3), ITS4 (5-TCCTCCGCTTATTGATATGC-3), and Taq DNA polymerase (Tiangen Biochemical Technology Co., Beijing, China) were used for the amplification of the Internal Transcribed Spacer (ITS) region using the PCR technique. The thermocyclic conditions were kept as initial denaturation at 94 °C for 5 min followed by 37 cycles of 94 °C for 1 min, 52 °C for 40 s, 72 °C for 1 min, and a final extension at 72 °C for 10 min [47]. Amplified DNA products were then sequenced from Beijing Genome Institute, China. The obtained sequences with accession numbers (OP984328, OP984329, OP984330, OP984331, OP984332, OP984333, and OP984334) were then BLAST searched at National Center for Biotechnology Information (NCBI) and closely related *Alternaria* species were retrieved from GenBank to carry out the phylogenetic analysis.

### 2.6. Pathogenicity Test of Alternaria solani

The inoculum for the pathogenicity test of each isolate was prepared from 10 days old culture grown on PDA media. Conidia suspension was harvested by flooding the plates with $ddH_2O$ containing 0.01% of surfactant Tween 20 and brushing the agar surface with a paintbrush. Leaves of two months old plants of moderately susceptible tomato variety Reograndi were sprayed with the prepared conidial suspension at $10^3$ $mL^{-1}$ rate until run-off. The data, including disease incidence (%), number of lesions/leaf, and lesion size ($mm^2$), were recorded at regular intervals after 5, 10, and 15 days of inoculation to select the highly virulent pathogen for further use and fulfilling Koch's postulate test.

### 2.7. In vitro Antifungal Studies of Silver Nanoparticles

Different concentrations of AgNPs, i.e., 5, 10, 15, 20, 25, and 50 ppm, were prepared to determine their effects on the growth of *A. solani.* The PDA media and 1 mL solution of different concentrations of AgNPs were poured down into respective Petri plates and incubated for 48 h. Petri plates were inoculated with an agar plug (placed in the center of each Petri plate) from pure culture and incubated at 27 ± 2 °C for 14 days. Three replicates were used to experiment, and no treatment was given to the control. The fungus growth was monitored regularly, and radial growth of the colony was noted after 14 days. The inhibition rate was calculated using the following equation.

$$\text{Rate of Inhibition } (\%) = \frac{R - r}{R} \times 100$$

where 'R' represents the radial growth of fungal mycelium in control plates, and 'r' is the radial growth of fungal mycelium in AgNPs treated plate [48].

### 2.8. Screening of Tomato Varieties against Alternaria solani

Earthen pots of 35.56 cm were washed, cleaned, and filled with a mixture of sandy and loamy soil in 1:3 ratio. Farmyard manure and DAP were added to the soil mixture to enrich it with nutrients. Pots were placed in a wired house covered with a plastic sheet to protect tomato plants from frosting. Already prepared seedlings of different varieties of tomato plants were transplanted in prepared pots, and leaves were sprayed with a conidial suspension of *A. salani* at a rate of $10^3$ $mL^{-1}$ in water until run-off [49]. Plants were irrigated regularly and monitored for the development of symptoms and severity of infection. The data were recorded after 15 days of inoculation.

The formula for the percentage of the Early Blight Index is given below.

$$\text{PEBI } (\%) = \frac{\text{Sum of all readings}}{\text{No. of leaves samped} \times \text{Maxi disease scale}} \times 100$$

EB severity on each leaf of the plants was recorded on a scale of 0 to 5, where 0 (immune) = no visible lesions on the leaf; 1 (highly resistant) = up to 10% leaf area affected; 2 (resistant) = 11–25%; 3 (tolerant) = 26–50%; 4 (susceptible) = 51–75%; and 5 (highly susceptibility) = more than 75% leaf area affected, or leaf abscised [50].

### 2.9. Greenhouse Experiment for In Vivo Efficacy of Silver Nanoparticles

A pot experiment was performed to determine the potential of AgNPs against the Early Blight disease of the tomato plant. Healthy seedlings of two susceptible varieties were transplanted into prepared pots and kept one plant per pot. The pots were arranged according to a randomized complete block design (RCBD). Leaves of plants were inoculated with *A. solani* and regularly monitored for the development of symptoms. Six different concentrations of AgNPs, 5, 10, 15, 20, 25, and 50 ppm, were prepared and applied as foliar spray twice at 15 days intervals on inoculated tomato plants. Tap water was given to plants taken as a negative control. Disease incidence, amount of phenols, and a few stress enzymes were recorded after 55 days of seedlings transplantation.

#### 2.9.1. Quantification of Total Phenolics

A test tube was taken and filled with 5 mL $dH_2O$, 1 mL methanolic leaf extract, and 250 mL Folin–Ciocalteu reagent (50% solution) and placed in the dark. After half an hour, 1 mL of 50% sodium carbonate ($Na_2CO_3$) solution was added and incubated for another 10 min in the dark. The absorption rate was determined at Δ725 nm using a double-beam spectrophotometer (BMS: 2800). Catechol was used to draw the standard curve. By comparing the standard curve, total phenolics were given as catechol μg $mg^{-1}$.

#### 2.9.2. Quantification of Peroxidases, Polyphenol Oxidases, and Phenylalanine Ammonia–Lyase

Leaves of treated plants (1 g) were crushed in a mortar containing ice-cold 100 mM phosphate buffer. The homogenized material with pH 7 was centrifuged at 4 °C for 15 min at 5000 rpm. The clear supernatant was collected and used to quantify enzymes.

Peroxidase activity was calculated using the Fu and Huang [51] method. Guaiacol reagent serving as the substrate was mixed with 10 mL sodium phosphate (10 mM) buffer. Finally, 3 mL of the enzyme mixture was added and incubated for 5 min at room temperature. At 470 nm, the absorbance was measured, and calculated PO activity was using Δ470 nm $gfw^{-1}$ $min^{-1}$ [50].

Polyphenol oxidase (PPO) was determined using the Mayer et al. [52] method. A total of 1.5 mL of sodium phosphate (10 mM) buffer (pH 6.0) was added to 150 mL of 0.1 M catechol solution (used as a substrate to measure enzyme activity). In this reaction mixture, 200 mL enzyme mixture was added and incubated for 1 h at room temperature. At Δ495 nm, the absorbance was measured, and PPO activity was estimated to be Δ495 nm $min^{-1}$ $mg^{-1}$ protein [51].

The Burrell and Rees [53] protocol was used to assess phenylalanine ammonia–lyase activity (PAL). L-phenylalanine (250 mL and 0.03 M) was added in 2.5 mL of sodium borate ($Na_2H_{20}B_4O_{17}$) buffer and 200 mL of the reaction mixture and maintained at pH 8.8. For 1 h, this reaction mixture was placed in a 37 °C water bath. After incubation, 1 M of trichloroacetic acid ($C_2HCl_3O_2$) solution was added, and the absorption rate was determined at Δ290 nm and measured in μg of trans-cinnamic acid $h^{-1}$ $mg^{-1}$ protein [52].

### *2.10. Data Analysis*

The data collected during lab and field work were evaluated by one-way analysis of variance (ANOVA). Duncan's multiple range test (DMRT) at 0.05% level of significance was used to separate the treatment means. PCA analysis was performed using Origin 2018 to determine the effect of AgNPs on growth attributes of tomato plant and correlation between disease incidence and other factors of plants studied.

## 3. Results

### *3.1. Characterization of Silver Nanoparticles*

The synthesis of silver nanoparticles was initially determined by color change. The yellow-colored reaction mixture changed to dark brown, indicating AgNP synthesis. Silver nanoparticles were then purified and subjected to UV–spectrophotometry. A clear and sharp characteristic peak at 424 nm giving an absorption rate of 0.368, can be seen in Figure 1a due to the surface plasmon resonance phenomenon verifying the synthesis of AgNPs. The particle size was recorded within 22–30 nm when subjected to Zeta sizer, as shown in Figure 1b.

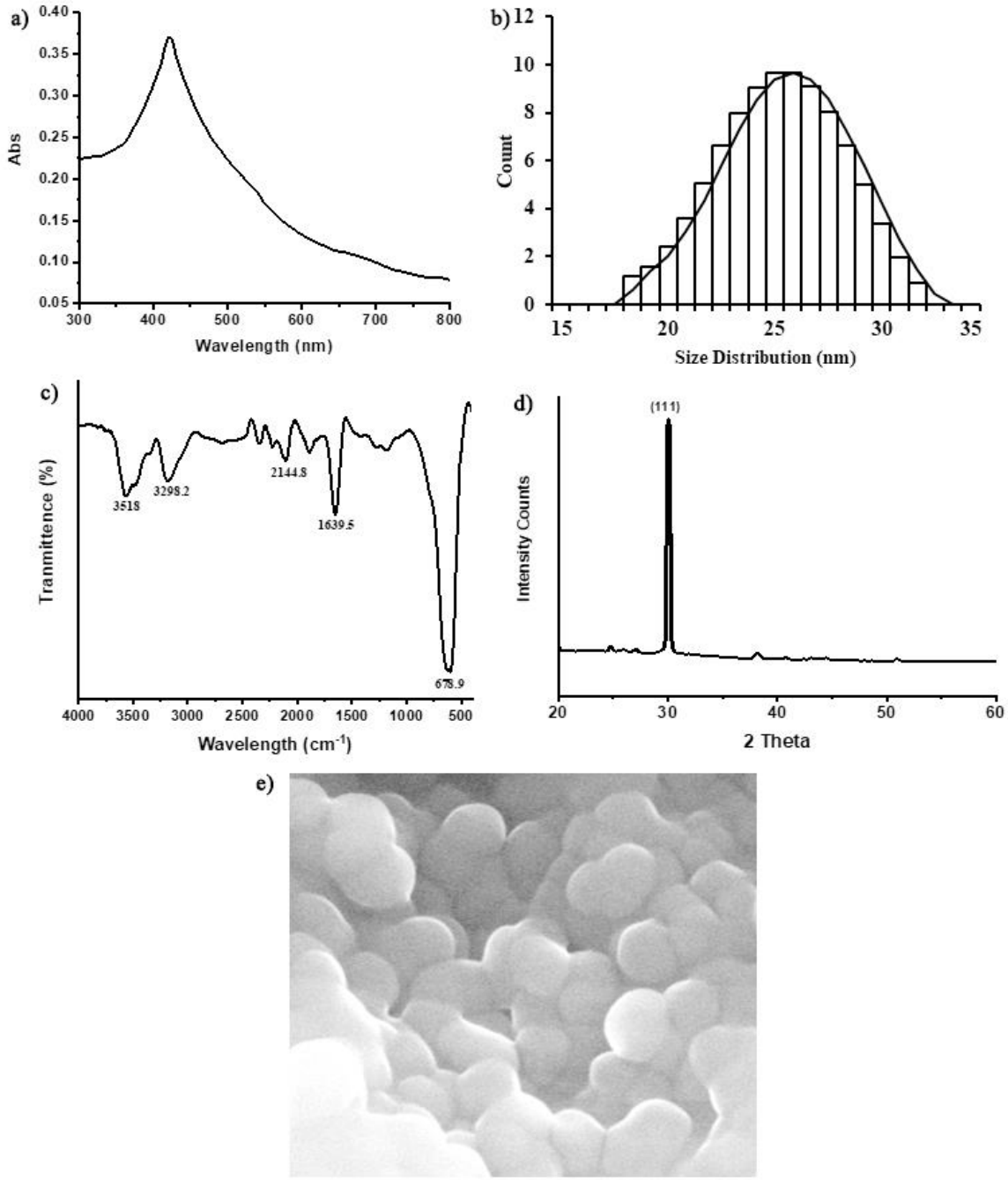


**Figure 1.** Physiochemical characterization of green synthesized silver nanoparticles using aqueous extract of Neem plant. (**a**) UV–spectrum (**b**) Size distribution using zeta sizer (**c**) FTIR spectrum (**d**) XRD spectrum and (**e**) SEM image.

FTIR analysis was performed to examine the attached functional groups of biomolecules on the surface of AgNPs acting as capping/stabilizing agents. The FTIR spectrum showed the absorption bands at 678.9 $cm^{-1}$, 1639.5 $cm^{-1}$, 2144.8 $cm^{-1}$, 3298.2 $cm^{-1,}$ and 3518 $cm^{-1}$ (Figure 1c). The peaks near 678.9 $cm^{-1}$ assigned to CH out of plane bending vibrations are substituted ethylene systems –CH=CH (cis). The band at 1639.5 $cm^{-1}$ corresponds to amide-I arising from carbonyl stretch –C=O) in proteins. The peaks at 2144.8 $cm^{-1}$ are assigned to the stretching vibration of –C–N of amide I, while the band at 3298.2 $cm^{-1}$ is assigned to C–H (methoxy compounds). The stretching vibration of aromatic compounds

and 3518 $cm^{-1}$ corresponds to –OH stretching vibration, indicating the presence of alcohol and phenol in capping and stabilizing AgNPs.

The XRD analysis indicates the synthesis of the crystalline nature of silver nanoparticles (Figure 1d). The size of samples was 24.98, determined using the Debye–Scherrer formula, with values close to the determined by the DLS technique by zeta sizer. A single sharp peak recorded at 2θ degrees of 30.06 is assigned to plane 111, suggesting a face-centered crystalline structure. A scanning electron microscope was used to study the surface morphology of green synthesized silver nanoparticles. Smooth and spherical AgNP nanoparticles can be seen in Figure 1e.

### *3.2. Morphological and Molecular Identification of Pathogen (Alternaria solani)*

The mycelial growth of all seven isolates was significantly diverse when grown on PDA media except for Shk-1 and Fsd-1. The growth range was between 48–70 mm in 7 days old culture, and maximum mycelial growth was shown by Bhl-1 (69.21 ± 0.090 mm) while minimum by M-1. The data of mycelial growth for all isolates, their color, and the nature of growth are given in Table 1. The conidia of isolates were straight, mostly oblong with a beak attached, and length without a beak varied between 13–24 µm. The conidia width was within the range of 7–12 µm, the minimum by M-1 (7.19 ± 0.565 µm), while the maximum was by Bhl-1 (12.81 ± 0.574 µm). The beak was straight to flexuous, and its length was more remarkable in Ksr-1 (23.15 ± 2.292 µm). The conidia of isolates had longitudinal (3–5 in Lhr-1, Ksr-1, Fsd-1, and M-1) and transverse septa (1–3 in Shk-1, Fsd-2, and Bhl-1). The color of conidia also varied from light to dark brown.

**Table 1.** Morphological characteristics of different *A. solani* isolates obtained from different areas of Punjab.

| Isolates | Colony Size (mm) | Colony Color | Mycelial Growth | Conidia Length (µm) | Conidia Width (µm) | Beak Length (µm) |
|---|---|---|---|---|---|---|
| Lhr-1 | 64.26 $^{e}$ ±0.188 | Whitish grey | Cottony Circular | 16.14 $^{c}$ ±0.866 | 9.29 $^{bc}$ ±1.641 | 19.56 $^{a}$ ±1.867 |
| Ksr-1 | 65.05 $^{d}$ ±0.159 | Whitish brown | Cottony Circular | 13.85 $^{c}$ ±2.066 | 7.66 $^{bc}$ ±0.613 | 23.15 $^{a}$ ±2.292 |
| Shk-1 | 68.59 $^{b}$ ±0.111 | Whitish brown | Cottony Circular | 21.20 $^{ab}$ ±1.170 | 10.61 $^{ab}$ ±0.924 | 17.63 $^{ab}$ ±0.918 |
| Fsd-1 | 68.56 $^{b}$ ±0.436 | Whitish brown | Cottony Circular | 23.33 $^{a}$ ±2.212 | 9.56 $^{bc}$ ±0.299 | 22.89 $^{a}$ ±0.966 |
| Fsd-2 | 66.01 $^{c}$ ±0.076 | Whitish brown | Cottony Circular | 18.21 $^{bc}$ ±1.141 | 8.51 $^{bc}$ ±1.164 | 11.77 $^{bc}$ ±0.681 |
| Bhl-1 | 69.21 $^{a}$ ±0.090 | Whitish grey | Cottony Circular | 23.68 $^{a}$ ±0.321 | 12.81 $^{a}$ ±0.574 | 6.53 $^{c}$ ±1.443 |
| M-1 | 48.21 $^{f}$ ±0.015 | Olive green | Not Cottony Circular | 16.27 $^{c}$ ±0.841 | 7.19 $^{c}$ ±0.565 | 13.18 $^{b}$ ±1.098 |

Treatment mean for each treatment is average of the three replicates; ± represents standard error; letters represent variation by isolates using Duncan's multiple range test.

Seven ITS sequences were obtained from seven isolates using ITS1 and ITS4 as forward and reverse primers. The homology analysis of the sequences retrieved from GenBank using the basic local alignment search tool (BLAST) and obtained sequences was performed. All the obtained sequences showed 99.5–99.7% identity with *Alternaria solani*. *Stemphylium sarciniforme* was chosen as the outgroup. The acquired and retrieved sequences were aligned using MAFFT software with default settings. The final data set contained 495 positions, of which 469 were conserved, 75 variable sites, 70 parsimony uninformative, and 31 informative. The maximum likelihood method, implemented in MEGA11 based on the Jukes–Cantor model, inferred the phylogenetic tree. In the phylogram, the obtained sequences clustered with different sequences of *Alternaria solani* have an identity of

99.1–99.5% in the same clade, supporting our morphological results (Figure 2). The results are based on ITS regions; further analyses could discriminate more clearly the isolates from other species, such as *A. tomatophila*.

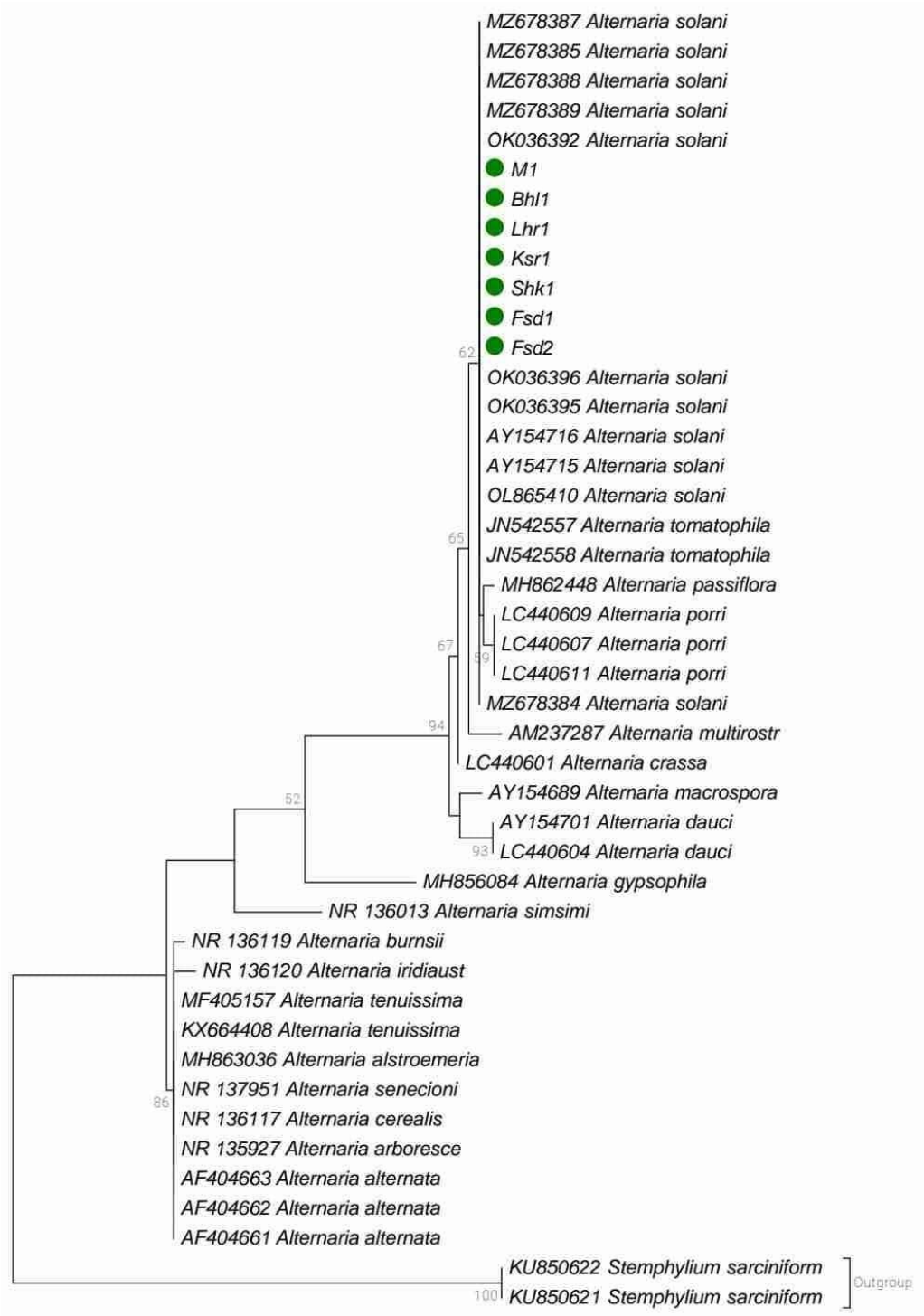


**Figure 2.** Phylogenetic analysis of amplified sequences by primer pair ITS (1 + 4) obtained from different isolates of *A. solani*.

### *3.3. Pathogenicity Variability among Alternaria solani Isolates*

The pathogenicity test for all seven isolates was conducted using a highly susceptible Rio Grande variety. The symptoms started appearing after three days of inoculation, but the data was recorded at regular intervals after 5, 10, and 15 days. The results revealed that

isolates Shk-1, Fsd-1, and Fsd-2 were highly virulent and severely attacked the plants. Other isolates, i.e., Lhr-1, Ksr-1, Bhl-1, and M-1, were also virulent, but their disease incidence was lesser than the isolates mentioned above. The percentage of disease incidence increased with time, and the maximum was by Shk-1 (88.22% ± 1.103) and the minimum by M-1 (69.69% ± 3.059) after 15 days of inoculation. There was no significant difference in the size and number of lesions that appeared on leaves, as given in Table 2.

**Table 2.** Pathogenicity study of each *A. solani* isolate against Rio Grande variety of tomato plant.

| Isolate Name | Disease Incidence (%) | | | No. of Lesions/Leaf | Size of Lesion ($mm^2$) | Virulency |
|---|---|---|---|---|---|---|
| | 5 Days | 10 Days | 15 Days | | | |
| Lhr-1 | 46.39 $^{cd}$ ±2.217 | 57.58 $^{cd}$ ±3.785 | 63.03 $^{d}$ ±2.389 | 5.00 $^{a}$ ±0.578 | 16.41 $^{a}$ ±2.132 | Virulent |
| Ksr-1 | 52.93 $^{b}$ ±1.070 | 63.54 $^{bc}$ ±1.470 | 76.17 $^{bc}$ ±1.875 | 5.67 $^{a}$ ±0.334 | 19.67 $^{a}$ ±2.502 | Virulent |
| Shk-1 | 61.69 $^{a}$ ±2.174 | 73.21 $^{a}$ ±2.566 | 88.22 $^{a}$ ±1.103 | 6.33 $^{a}$ ±0.883 | 20.77 $^{a}$ ±2.299 | Highly Virulent |
| Fsd-1 | 51.00 $^{bc}$ ±0.958 | 69.54 $^{ab}$ ±2.058 | 85.58 $^{ab}$ ±4.616 | 6.00 $^{a}$ ±0.578 | 21.16 $^{a}$ ±1.860 | Highly Virulent |
| Fsd-2 | 48.43 $^{bcd}$ ±1.681 | 68.37 $^{ab}$ ±3.278 | 85.60 $^{ab}$ ±3.640 | 6.67 $^{a}$ ±0.667 | 20.48 $^{a}$ ±0.168 | Highly Virulent |
| Bhl-1 | 52.52 $^{b}$ ±0.667 | 69.62 $^{ab}$ ±2.935 | 75.32 $^{c}$ ±3.771 | 5.33 $^{a}$ ±0.667 | 19.24 $^{a}$ ±0.688 | Virulent |
| M-1 | 44.48 $^{d}$ ±2.496 | 54.70 $^{d}$ ±0.818 | 69.69 $^{cd}$ ±3.059 | 5.67 $^{a}$ ±0.334 | 18.86 $^{a}$ ±1.199 | Virulent |

Treatment mean for each treatment is average of the three replicates; ± represents standard error; letters represent variation by isolates using Duncan's multiple range test.

### *3.4. In Vitro Antifungal Analysis of Silver Nanoparticles against Alternaria solani*

Silver nanoparticles have shown antifungal activity and proved to be a potential fungicide against each isolate, inhibiting 70–80% growth, as shown in Figures 3 and 4. The inhibition rate increased gradually as the concentration of silver nanoparticles increased from 5 to 50 ppm. The silver nanoparticles showed the maximum rate of inhibition against Shk-1, i.e., 81.10% compared to control, followed by Fsd-2 (79.39%), Bhl-1 (78.51%), Ksr-1 (76.97%), Lhr-1 (76.33%), Fsd-1 (75.34%), and M-1 (65.44%).

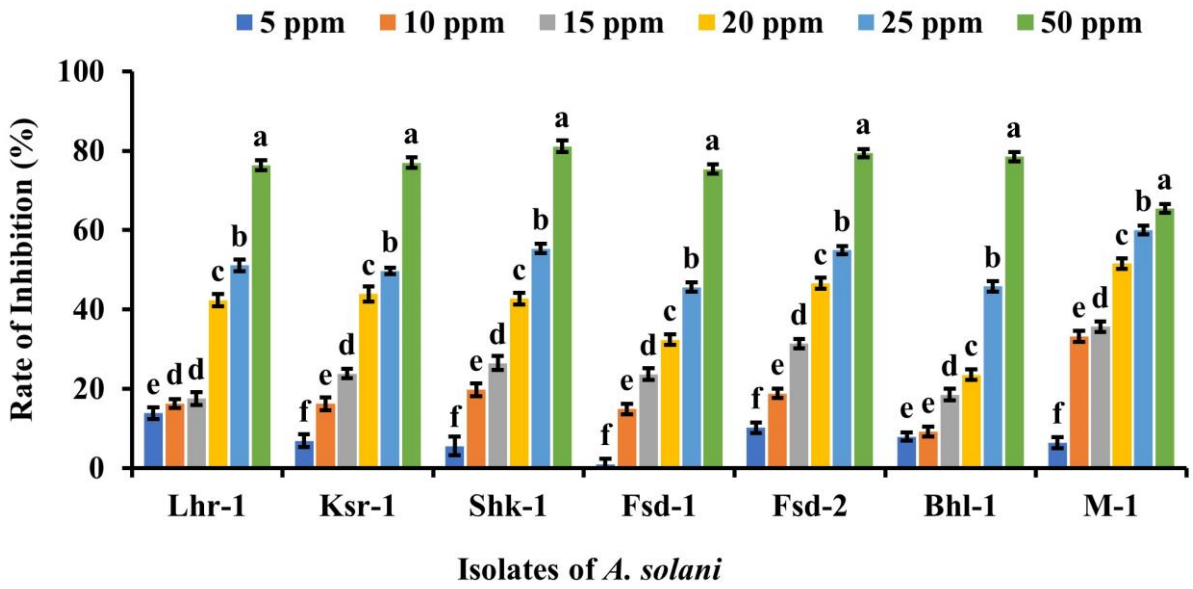


**Figure 3.** Antifungal activity of green synthesized silver nanoparticles against different isolates of *A. solani* letters represent variation by treatments using Duncan's multiple range test.

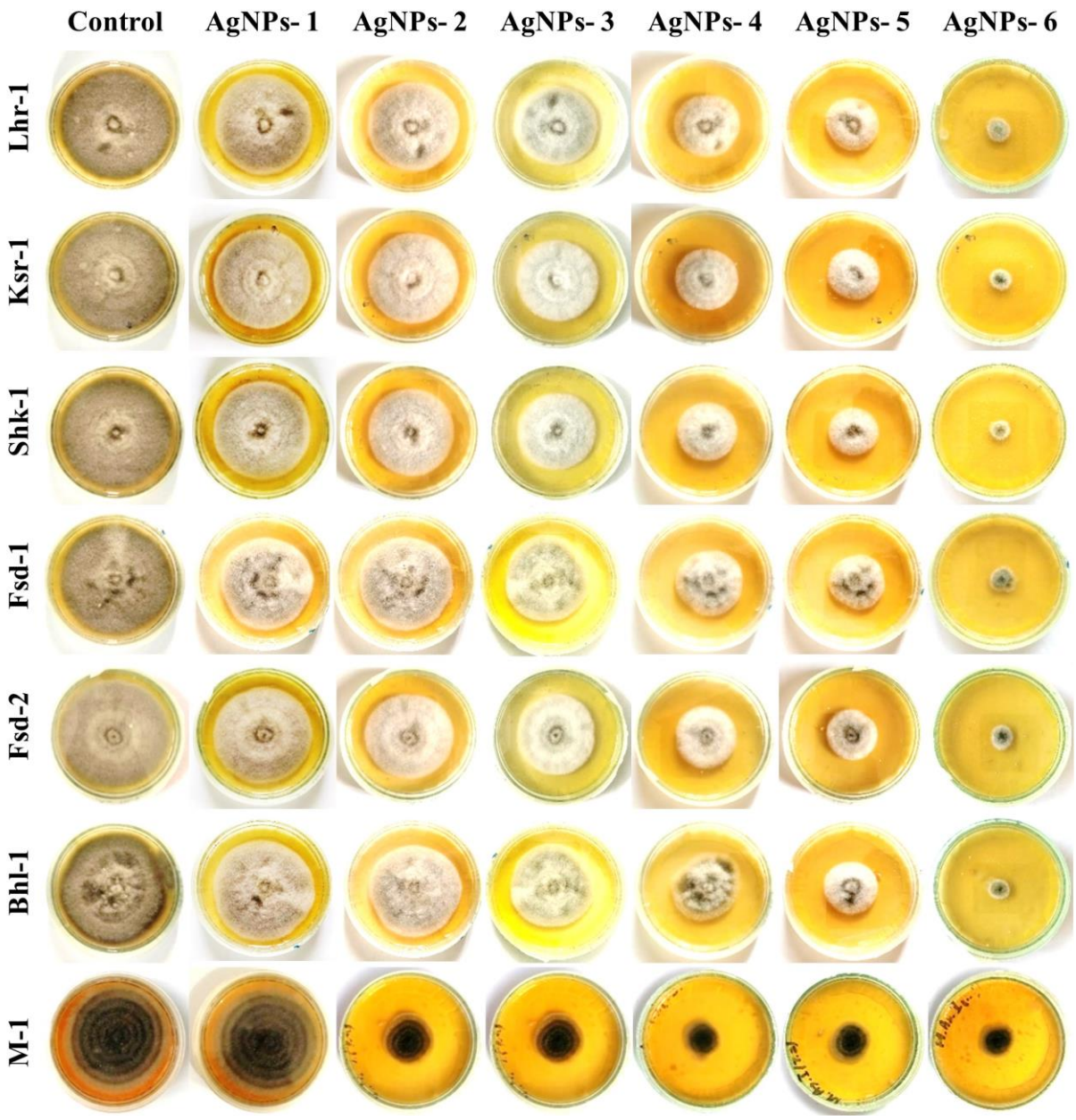


**Figure 4.** Effect of green synthesized silver nanoparticles on radial growth of different isolates of *A. solani*. Analysis was performed after 14 days of incubation.

### *3.5. Screening of Susceptible Tomato Varieties against Alternaria solani*

Six local and six hybrid varieties obtained from Ayyub Agriculture Research Institute, Faisalabad, Roshan seeds, Lahore, and Sheikhupura were tested against a highly virulent isolate, Shk-1 (Figure 5). The plants showed symptoms during the early stage of infection, but the data were recorded after 15 days of inoculation. Nagina and Red diamond varieties were tolerant against the Shk-1 isolate, showing 38.67% and 39.33% disease index, respectively. The other six varieties, Roma, Sultan, Sahel, Amber, Red stone, and Clara, were ranked as susceptible with 48%, 56%, 54.67%, 50.67%, 45%, and 40.67% disease index, respectively. Naqeeb was the highly susceptible variety, with an 80% disease index, followed by Nadar (74.67%), Rio Grande (73.33%), and Cristal (66.67%). The plants of the Naqeeb variety were highly injured, with 56.62% tissue damage. Infection also highly occurred among the Rio Grande, Sultan, and Cristal variety plants. There was a significant difference between lesions size appearing on different tomato varieties given in Table 3.

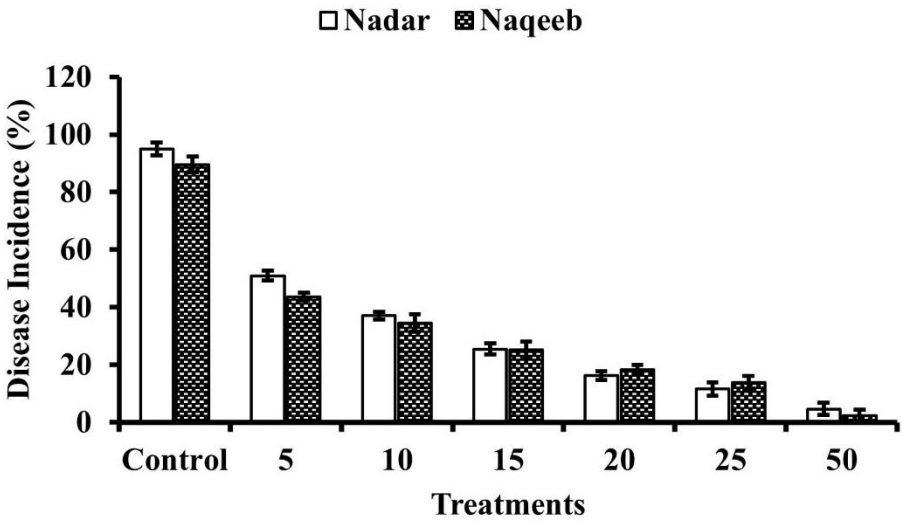


**Figure 5.** Disease suppression efficacy of green synthesized silver nanoparticles against Early Blight of tomato plants. Disease incidence (%) was recorded after 15 days of inoculation.

**Table 3.** Response of different tomato varieties against *A. solani*.

| Varieties | Parameters | No. of Lesions per Leaf | Size of Lesion ($mm^2$) | Infected Area of Leaf (%) | Disease Incidence (%) | Disease Index (%) | Disease Reaction |
|---|---|---|---|---|---|---|---|
| Local Varieties | Nadar | 5.07 $^{b}$ ±0.372 | 23.20 $^{def}$ ±1.656 | 38.24 $^{bc}$ ±0.614 | 47.12 $^{c}$ ±2.935 | 74.67 $^{bc}$ ±1.766 | Highly Susceptible |
| | Naqeeb | 6.00 $^{a}$ ±0.116 | 30.14 $^{bc}$ ±1.063 | 54.98 $^{a}$ ±0.694 | 56.62 $^{a}$ ±3.636 | 80.00 $^{a}$ ±2.312 | Highly Susceptible |
| | Nagina | 3.80 $^{cd}$ ±0.347 | 25.40 $^{cde}$ ±1.731 | 29.16 $^{efg}$ ±1.223 | 28.06 $^{fg}$ ±0.502 | 38.67 $^{g}$ ±3.532 | Tolerant |
| | Roma | 3.27 $^{d}$ ±0.176 | 41.61 $^{efg}$ ±0.301 | 35.28 $^{bcd}$ ±2.849 | 25.10 $^{fgh}$ ±3.443 | 48.00 $^{ef}$ ±2.312 | Susceptible |
| | Rio Grande | 6.00 $^{a}$ ±0.2 | 41.53 $^{a}$ ±3.729 | 33.77 $^{cde}$ ±0.799 | 52.31 $^{ab}$ ±3.339 | 73.33 $^{b}$ ±1.335 | Highly Susceptible |
| | Sultan | 4.20 $^{c}$ ±0.116 | 34.13 $^{b}$ ±2.835 | 26.58 $^{fg}$ ±1.018 | 40.44 $^{cd}$ ±2.233 | 56.00 $^{d}$ ±2.312 | Susceptible |
| | Sahel | 3.67 $^{cd}$ ±0.133 | 26.87 $^{cd}$ ±3.325 | 36.81 $^{bcd}$ ±0.727 | 31.58 $^{ef}$ ±1.878 | 54.67 $^{de}$ ±2.669 | Susceptible |
| Hybrid Varieties | Cristal | 4.07 $^{c}$ ±0.176 | 29.36 $^{bcd}$ ±1.474 | 39.96 $^{b}$ ±4.139 | 45.71 $^{bc}$ ±0.371 | 66.67 $^{c}$ ±1.337 | Highly Susceptible |
| | Amber | 4.13 $^{c}$ ±0.291 | 17.82 $^{fg}$ ±0.367 | 31.59 $^{def}$ ±1.763 | 30.01 $^{fg}$ ±1.525 | 50.67 $^{def}$ ±1.335 | Susceptible |
| | Red Stone | 4.33 $^{c}$ ±0.241 | 16.76 $^{g}$ ±1.135 | 24.27 $^{g}$ ±2.505 | 23.74 $^{gh}$ ±2.305 | 45.33 $^{fg}$ ±2.669 | Susceptible |
| | Red Diamond | 3.37 $^{d}$ ±0.145 | 17.03 $^{fg}$ ±1.422 | 17.74 $^{h}$ ±0.894 | 18.98 $^{h}$ ±0.809 | 39.33 $^{g}$ ±2.909 | Tolerant |
| | Clara | 3.30 $^{d}$ ±0.067 | 18.27 $^{fg}$ ±0.754 | 31.54 $^{def}$ ±0.683 | 25.52 $^{fgh}$ ±0.656 | 40.67 $^{g}$ ±1.335 | Susceptible |

Treatment mean for each treatment is average of the three replicates; ± represents standard error; letters represent variation by verities using Duncan's multiple range test.

### *3.6. In Vivo Efficacy of Silver Nanoparticles against A. solani*

Different concentrations of silver nanoparticles, 5, 10, 15, 20, 25, and 50 ppm, demonstrated an effective reduction in disease incidence compared to the control. The disease was reduced from 50% to 5% in both varieties by increasing the concentration of silver nanoparticles from 5 ppm to 50 ppm. The plants exposed to the pathogen showed more than 80% disease incidence compared to plants treated with silver nanoparticles. The amount of phenolics compounds, PAL, PO, and PPO, was also quantified. The amount of

phenolic compound was significantly increased in silver nanoparticles treated plants at lower concentrations than in control. The production decreased at a higher concentration of silver nanoparticles but was more than the control (Figure 6a). The PO activity increased in treated tomato plants in the same way that phenolic activity increased. Lower concentrations of silver nanoparticles resulted in the highest PO activity in Nadar and Naqeeb (Figure 6b). The most increased activity was observed at 5 and 10 ppm compared to the control. Other concentrations ranging from 15 to 20 ppm exhibited 25% and 10% more activity than control in both varieties. However, activity was comparatively reduced at 25 and 50 ppm.

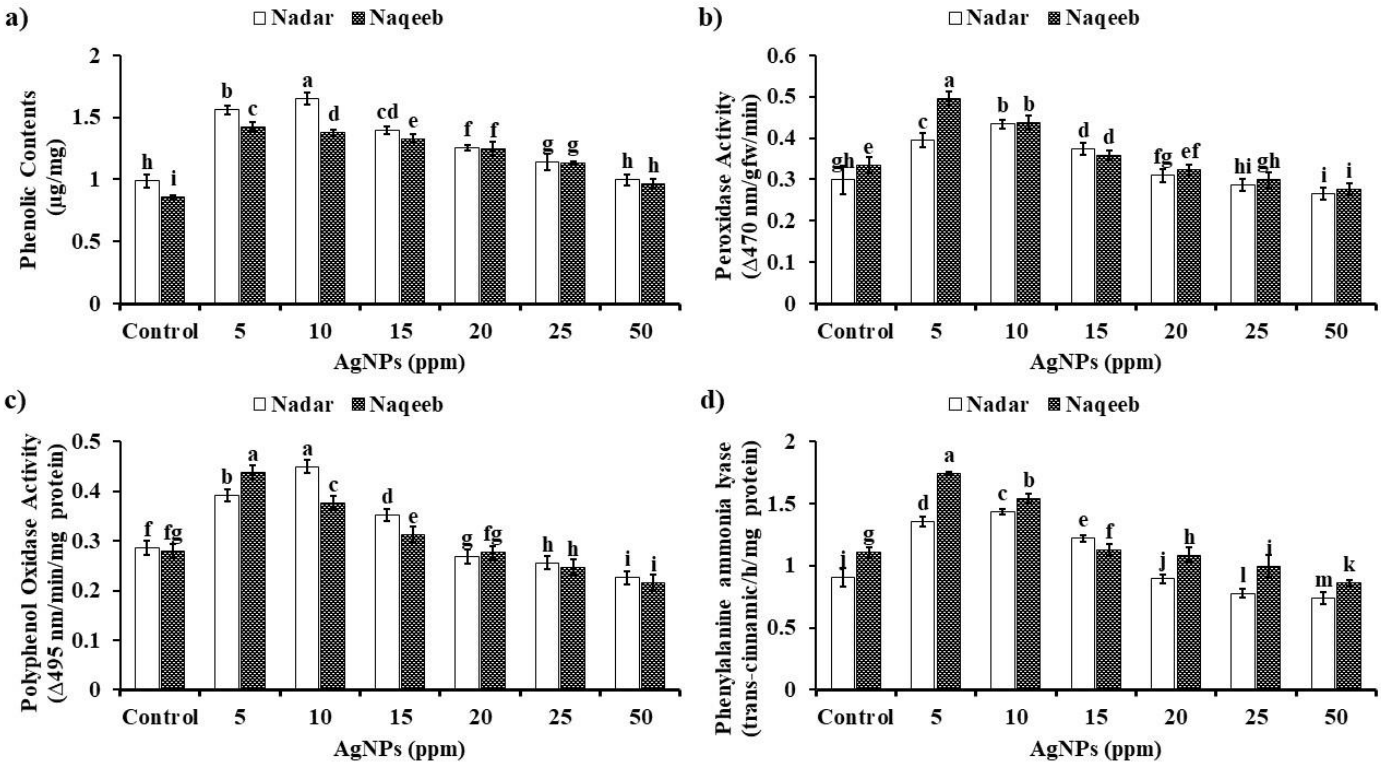


**Figure 6.** Effect of green synthesized silver nanoparticles on disease-related compounds of tomato plants. Quantification was performed after 55 days of seedling transplantation. (**a**) Phenolic content, (**b**) Peroxidase (PO) activity, (**c**) Polyphenol oxidase activity, and (**d**) Phenylalanine ammonia–lyase (PAL) activity. Letters represent variation by treatments using Duncan's multiple range test.

In the case of PPO activity, it was found in excess in tomato plants with lower concentrations of AgNPs (Figure 6c). Various concentration ranges from 5 to 15 ppm exhibited 20–60% activity in Nadar and 10–60% activity in Naqeeb, with maximum activity observed at 10 ppm (0.449±0.013 Δ495 nm/min/mg protein) in Nadar and 5 ppm (0.437±0.014 Δ495 nm/min/mg protein) in Naqeeb. PPO activity was lower at higher concentrations, i.e., 20, 25, and 50 ppm, than the control. These findings suggested that AgNPs could increase PPO activity, allowing plants to fight pathogenic stress and grow healthy. In plants treated with AgNPs, the same pattern was observed for PAL activity (Figure 6d). Plants treated with lower concentrations of silver nanoparticles showed increased PAL activity compared to the control. In comparison, plants treated with higher concentrations of silver nanoparticles showed the least PAL activity.

### *3.7. Principal Component Analysis (PCA)*

Data variability of 95.71% (PC1 = 70.72%, PC2 = 24.99%) was revealed by PCA, as shown in Figure 7. Disease indices and growth rate of the pathogen on leaves were negatively correlated with phenolic compounds, PO, PPO, and PAL. The foliar application

of 5 and 10 ppm of silver nanoparticles was most effective in crop protection, enhancing the defective mechanism and reducing the pathogen growth.

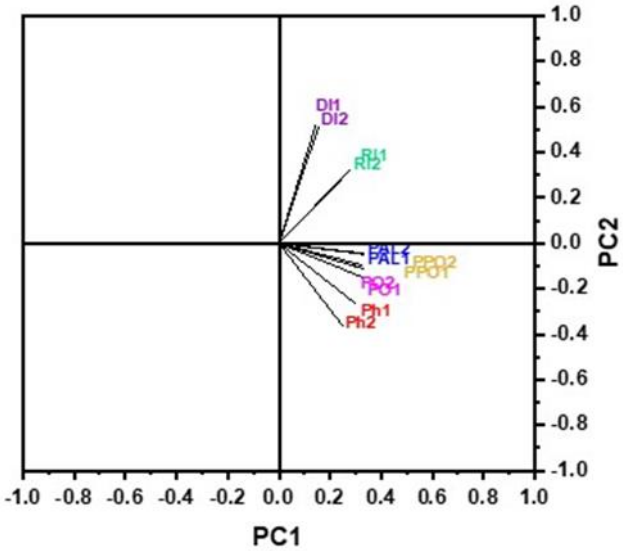


**Figure 7.** Principal component analysis (PCA) showing the effect of AgNPs on various attributes of two tomato varieties (Nadar as 1 and Naqeeb 2) infected with *A. solani*, DI= disease incidence, RI = rate of growth of pathogen, Ph = Phenolics compounds, PO = peroxidase activity, PPO = polyphenol peroxidase activity, PAL = Phenylalanine ammonia–lyase activity.

## 4. Discussion

Green nanoparticle synthesis is a more advanced, widespread, and remarkable area of nanotechnology [54]. Using plants to synthesize nanoparticles is easy, single-step, non-pathogenic, cost-effective, non-toxic, and sustainable as it uses renewable recourses and is environment friendly [10,55]. Various plants like neem [56,57], moringa [58], java plum [59], fig, rosemary [60], and many others have been reported to be used in the synthesis of silver nanoparticles. Silver nanoparticles possess unique optical properties due to surface plasmon resonance (SPR) generated from free electron movement. Therefore, interact with a specific wavelength of visible light reported between 400–500 nm and develops brown color in the solution depicting the synthesis of silver nanoparticles [61–63]. In the current study, AgNPs of 22–30 nm size and spherical shape were synthesized using leaves extract of the Neem plant and evaluated for their antifungal activity against *Alternaria solani*. The absorption peak of the AgNPs synthesized was also shown at 424 nm. FTIR analysis makes us understand the role of biomolecules in plant leaf extract for reducing silver to silver nanoparticles and acting as capping agents [64]. The FTIR analysis reveals the involvement of alkanes, alkynes, amines, carboxylic groups [65], methylene [66], and various other biomolecules in reducing and stabilizing green synthesized silver nanoparticles [67]. XRD pattern and SEM analysis of AgNPs synthesized by neem and other plants also suggest the synthesis of crystalline structure spherical silver nanoparticles [68–70]. Mohamed and Elshahawy [71] synthesized silver nanoparticles of 32–47 size using peel extract of orange (*Citrus sinensis* L.). UV–Vis spectrum showed an absorption peak at 435 nm corresponding to silver nanoparticles [66]. Chakravarty et al. [59] synthesized spherical-shaped silver nanoparticles using fruit extract of *Syzygium cumini* L., which showed a characteristic peak at 443 nm. The presence of OH and C=O confirmed the presence of secondary plant metabolites by FTIR spectroscopy. Green synthesized nanoparticles have tremendous biological applications in medicine and agriculture as antibacterial, antifungal, and anti-cancerous agents [72,73]. The current findings highlight the importance of green synthesized silver nanoparticles in disease reduction. Early Blight disease of tomatoes is widespread worldwide and devastatingly causes massive crop yield loss yearly. In the present study, we successfully isolated and identified *A. solani*, responsible for Early Blight disease in tomato

plants. The identification of the pathogen is important for developing effective disease management strategies. The colony color, pattern, and muriform conidia with beak confirmed the presence of *A. solani*, and the variation among different isolates was seen clearly. The molecular characterization using PCR amplification and sequencing of the ITS region of the genome confirmed the identification of the isolated fungus as *A. solani*, with 99% sequence similarity to the *A. solani* reference sequences. The results of this study indicated that *A. solani* was highly pathogenic to tomato plants, causing significant damage to both the leaves and the fruits. The symptoms of Early Blight disease caused by *A. solani* included the formation of brown, circular lesions with concentric rings on the plant's leaves. The virulence factors produced by *A. solani* allow the fungus to invade and colonize the plant tissues, leading to disease symptoms. The cultural, morphological, and genetic variability of *A. solani,* their virulency among different isolates, and resistance in some tomato varieties have been reported in recent decades. Riaz et al. [74] revealed the morphological and genetic variation among different isolates of *A. solani* in various areas of Punjab, Pakistan. All isolates showed radial growth, colony character, and conidial morphology variation. A field survey revealed the variation ranging from 9–74% incidence with 6.11–24% severity among different areas of Punjab, Pakistan [74]. Disease severity and incidence are so high in various regions because of continuous farming without rotation of crops, lack of proper disease management, and uninterrupted and rigorous farming. Lack of awareness among farmers has introduced genetic variation and resistant pathogens because of the unlimited use of fungicides due to lack of awareness among farmers [75–77]. Isolation and identifying actual disease pathogens could be fundamental tools for understanding disease progression and exploring the curative agents. As genus *A. solani* poses a significant threat to vegetables nowadays, thus it is of utmost importance to identify its different species to explore potential control measures [78]. Riaz et al. [74] also collected different isolates of *A. solani,* which showed smooth, circular, and greenish-black colony growth with variations in size. The conidia were single, usually flexuous or straight, with beak attached varied in size within the range of 68 to 88 µm [74].

Disease severity also depends upon the level of pathogenicity and its variation among different isolates of *A. solani* [79,80], as shown in the present study and a few previous reports [49,81,82]. It has become essential to control these resistant pathogens effectively using various methods [83]. Scientists have reported using green synthesized silver nanoparticles as a promising tool against different phytopathogenic fungi as a more effective substitute for synthetic fungicides commonly used by farmers [84–86]. Silver nanoparticles prepared using orange peel and pomegranate extract inhibited the mycelial growth of *A. solani* by almost 60–80% when treated with different concentrations [87]. Tyagi et al. [32] also reported in 2020 that biosynthesized nanoparticles can inhibit the absolute growth (100%) of *A. solani* at 100 ppm concentration. However, the inhibition rate varies with the change in the concentration of silver nanoparticles. Silver nanoparticles probably disrupt DNA replication and inactivate the functions of cellular proteins and enzymes, preventing the normal functioning of the pathogen [31,88]. Silver nanoparticles inhibit pathogen growth, prevent plants from establishing infection, and combat collateral damage [89]. The main components of several anti-pathogenic compounds secreted by plants, which serve as the first line of defense, are phenolic compounds. Silver nanoparticles stimulate the production of phenols in plants, which aids in the reduction of disease severity [90]. Foliar application of biosynthesized silver nanoparticles improved tomato plants' first line of defense, as evidenced by increased phenolics and antioxidative enzyme production (PO, PPO, and PAL). Plants with increased resistance are better prepared to reduce ROS production after a pathogen attack, resulting in lower stress enzyme activity in plants treated with silver nanoparticles [91].

## 5. Conclusions

Early Blight disease of the tomato plant is a serious challenge for farmers, which affects crop yield due to pathogen variability. The identification and occurrence of *A. solani*

in tomato crops were also investigated in the current study. The results showed that the pathogen is prevalent in tomato crops, highlighting the importance of developing effective disease management strategies. Green synthesized nanomaterials are a safe and effective alternative to chemical fungicides in controlling Early Blight disease and are regarded as the best option in this scenario. Green synthesis is a simple, environment-friendly, cost-effective, and easily scaled procedure for the large-scale synthesis of nanoparticles. The application of silver nanoparticles reduced the pathogenic growth of *A. solani* depending on the concentration. The different treatments of silver nanoparticles on tomato leaves increased the resistance in plants by producing phenolics and other antioxidants. Silver nanoparticles can be used for managing diseases, rapid disease detection, and enhancing the ability of plants to absorb nutrients. The findings of this study have significant implications for the development of safe and sustainable plant disease management strategies that can minimize the use of chemical fungicides and promote eco-friendly agricultural practices. Using green synthesized silver nanoparticles as an antifungal agent can reduce the risk of environmental pollution and toxicity associated with chemical fungicides. Overall, this study adds to the research on the behavior of nanoparticles in the ecosystem by providing important information about the effects of silver nanoparticles on plant oxidative responses.

**Author Contributions:** Conceptualization, M.A., S.A., A.A. and M.T.K.; methodology, M.A. and S.A.; software, S.A., A.A., A.I. and I.M.; validation, S.A. and M.T.K.; formal analysis, A.A. and I.M; investigation, S.A. and M.A.; resources, S.A. and M.A.; data curation, A.A., I.K.J. and M.T.K.; writing—original draft preparation, M.A., A.A., H.M.A., N.A.H. and M.E.H.; writing—review and editing, H.M.A., N.A.H., M.E.H., S.A., A.A. and I.K.J.; visualization, M.A., A.A. and A.I.; supervision, S.A.; project administration, H.M.A.; funding acquisition, H.M.A., N.A.H. and M.E.H. All authors have read and agreed to the published version of the manuscript.

**Funding:** This work was funded by the Researchers Supporting Project number (RSP2023R123), King Saud University, Riyadh, Saudi Arabia.

**Data Availability Statement:** The original contributions presented in the study are included in the article. Further inquiries can be directed to the corresponding author.

**Acknowledgments:** Authors would like to extend their sincere appreciation to the Researchers Supporting Project number (RSP2023R123), King Saud University, Riyadh, Saudi Arabia.

**Conflicts of Interest:** The authors declare no conflict of interest.

## References

1. Bayda, S.; Adeel, M.; Tuccinardi, T.; Cordani, M.; Rizzolio, F. The history of nanoscience and nanotechnology: From chemical–physical applications to nanomedicine. *Molecules* **2019**, *25*, 112. [CrossRef] [PubMed]
2. Sharma, M.; Chauhan, P.; Sharma, R.; Kumar, D. Application of Nanotechnology in Clinical Research: Present and Future Prospects. In *Nanomaterials in Clinical Therapeutics: Synthesis and Applications*; Wiley: Hoboken, NJ, USA, 2022; pp. 75–113.
3. Findik, F. Nanomaterials and their applications. *Period. Eng. Nat. Sci.* **2021**, *9*, 62–75. [CrossRef]
4. Das, R.K.; Pachapur, V.L.; Lonappan, L.; Naghdi, M.; Pulicharla, R.; Maiti, S.; Cledon, M.; Dalila, L.M.A.; Sarma, S.J.; Brar, S.K. Biological synthesis of metallic nanoparticles: Plants, animals and microbial aspects. *Nanotechnol. Environ. Eng.* **2017**, *2*, 18. [CrossRef]
5. Wang, H.; Wan, K.; Shi, X. Recent advances in nanozyme research. *Adv. Mater.* **2019**, *31*, 1805368. [CrossRef]
6. Narayanan, M.; Devarajan, N.; He, Z.; Kandasamy, S.; Ashokkumar, V.; Raja, R.; Carvalho, I.S. Assessment of microbial diversity and enumeration of metal tolerant autochthonous bacteria from tailings of magnesite and bauxite mines. *Materials* **2020**, *33*, 4391–4401. [CrossRef]
7. Haq, I.U.; Khurshid, A.; Inayat, R.; Kexin, Z.; Changzhong, L.; Ali, S.; Zuan, A.T.K.; Al-Hashimi, A.; Abbasi, A.M. Silicon-based induced resistance in maize against fall armyworm [*Spodoptera frugiperda* (Lepidoptera: Noctuidae)]. *PLoS ONE* **2021**, *16*, e0259749. [CrossRef]
8. Subramaniam, S.; Kumarasamy, S.; Narayanan, M.; Ranganathan, M.; Rathinavel, T.; Chinnathambi, A.; Alahmadi, T.A.; Karuppusamy, I.; Pugazhendhi, A.; Whangchai, K. Spectral and structure characterization of Ferula assafoetida fabricated silver nanoparticles and evaluation of its cytotoxic, and photocatalytic competence. *Environ. Res.* **2022**, *204*, 111987. [CrossRef]
9. Haq, I.U.; Zhang, K.; Ali, S.; Majid, M.; Ashraf, H.J.; Khurshid, A.; Inayat, R.; Li, C.; Gou, Y.; Al-Ghamdi, A.A. Effectiveness of silicon on immature stages of the fall armyworm [*Spodoptera frugiperda* (JE Smith)]. *J. King Saud Univ. Sci.* **2022**, *34*, 102152. [CrossRef]

10. Thummaneni, C.; Prakash, D.S.; Golli, R.; Vangalapati, M. Green synthesis of silver nanoparticles and characterization of caffeic acid from Myristica fragrans (Nutmeg) against antibacterial activity. *Mater. Today: Proc.* **2022**, *62*, 4001–4005. [CrossRef]
11. Chattha, M.U.; Amjad, T.; Khan, I.; Nawaz, M.; Ali, M.; Chattha, M.B.; Ali, H.M.; Ghareeb, R.Y.; Abdelsalam, N.R.; Azmat, S. Mulberry based zinc nano-particles mitigate salinity induced toxic effects and improve the grain yield and zinc bio-fortification of wheat by improving antioxidant activities, photosynthetic performance, and accumulation of osmolytes and hormones. *Front. Plant Sci.* **2022**, *13*, 920570. [CrossRef]
12. Salem, S.S.; Fouda, A. Green synthesis of metallic nanoparticles and their prospective biotechnological applications: An overview. *Biol. Trace Elem. Res.* **2021**, *199*, 344–370. [CrossRef]
13. Khan, I.; Saeed, K.; Khan, I. Nanoparticles: Properties, applications and toxicities. *Arab. J. Chem.* **2019**, *12*, 908–931. [CrossRef]
14. Bhuyar, P.; Rahim, M.H.A.; Sundararaju, S.; Ramaraj, R.; Maniam, G.P.; Govindan, N. Synthesis of silver nanoparticles using marine macroalgae *Padina* sp. and its antibacterial activity towards pathogenic bacteria. *Beni-Suef Univ. J. Basic Appl. Sci.* **2020**, *9*, 1–15. [CrossRef]
15. Ijaz, I.; Gilani, E.; Nazir, A.; Bukhari, A. Detail review on chemical, physical and green synthesis, classification, characterizations and applications of nanoparticles. *Green Chem Lett. Rev.* **2020**, *13*, 223–245. [CrossRef]
16. Rizwan, M.; Hussain, M.; Rauf, A.; Zafar, M.N.; Mabkhot, Y.N.; Maalik, A. Green synthesis and antimicrobial evaluation of silver nanoparticles mediated by leaf extract of *Syzygium cumini* against poultry pathogens. *Micro Nano Lett.* **2020**, *15*, 600–605. [CrossRef]
17. Akpinar, I.; Unal, M.; Sar, T. Potential antifungal effects of silver nanoparticles (AgNPs) of different sizes against phytopathogenic *Fusarium oxysporum* f. sp. radicis-lycopersici (FORL) strains. *SN Appl. Sci.* **2021**, *3*, 506. [CrossRef]
18. Ghareeb, R.Y.; Shams El-Din, N.G.E.-D.; Maghraby, D.M.E.; Ibrahim, D.S.; Abdel-Megeed, A.; Abdelsalam, N.R. Nematicidal activity of seaweed-synthesized silver nanoparticles and extracts against *Meloidogyne incognita* on tomato plants. *Sci. Rep.* **2022**, *12*, 3841. [CrossRef] [PubMed]
19. Wang, L.; Ali, J.; Zhang, C.; Mailhot, G.; Pan, G. Simultaneously enhanced photocatalytic and antibacterial activities of TiO2/Ag composite nanofibers for wastewater purification. *J. Environ. Chem. Eng.* **2020**, *8*, 102104. [CrossRef]
20. Shah, S.S.; Shaikh, M.N.; Khan, M.Y.; Alfasane, M.A.; Rahman, M.M.; Aziz, M.A. Present status and future prospects of jute in nanotechnology: A review. *Chem. Rec.* **2021**, *21*, 1631–1665. [CrossRef] [PubMed]
21. Nongbet, A.; Mishra, A.K.; Mohanta, Y.K.; Mahanta, S.; Ray, M.K.; Khan, M.; Chakrabartty, I. Nanofertilizers: A Smart and Sustainable Attribute to Modern Agriculture. *Plants* **2022**, *11*, 2587. [CrossRef]
22. Sadak, M.S. Impact of silver nanoparticles on plant growth, some biochemical aspects, and yield of fenugreek plant (*Trigonella foenum-graecum*). *Bull. Natl. Res. Cent.* **2019**, *43*, 38. [CrossRef]
23. Hernández-Díaz, J.A.; Garza-García, J.J.; Zamudio-Ojeda, A.; León-Morales, J.M.; López-Velázquez, J.C.; García-Morales, S. Plant-mediated synthesis of nanoparticles and their antimicrobial activity against phytopathogens. *J. Sci. Food Agric.* **2021**, *101*, 1270–1287. [CrossRef]
24. Skłodowski, K.; Chmielewska-Deptuła, S.J.; Piktel, E.; Wolak, P.; Wollny, T.; Bucki, R. Metallic Nanosystems in the Development of Antimicrobial Strategies with High Antimicrobial Activity and High Biocompatibility. *Int. J. Mol. Sci.* **2023**, *24*, 2104. [CrossRef]
25. Patil, S.; Singh, N. Antibacterial silk fibroin scaffolds with green synthesized silver nanoparticles for osteoblast proliferation and human mesenchymal stem cell differentiation. *Colloids Surf. B: Biointerfaces* **2019**, *176*, 150–155. [CrossRef] [PubMed]
26. Hariram, M.; Vivekanandhan, S.; Ganesan, V.; Muthuramkumar, S.; Rodriguez-uribe, A.; Mohanty, A.; Misra, M. Tecoma stans flower extract assisted biogenic synthesis of functional Ag-Talc nanostructures for antimicrobial applications. *Bioresour. Technol.* **2019**, *7*, 100298. [CrossRef]
27. Takáč, P.; Michalková, R.; Čižmáriková, M.; Bedlovičová, Z.; Balážová, Ľ.; Takáčová, G. The Role of Silver Nanoparticles in the Diagnosis and Treatment of Cancer: Are There Any Perspectives for the Future? *Life* **2023**, *13*, 466. [CrossRef] [PubMed]
28. Afkhami, F.; Forghan, P.; Gutmann, J.L.; Kishen, A. Silver Nanoparticles and Their Therapeutic Applications in Endodontics: A Narrative Review. *Pharmaceutics* **2023**, *15*, 715. [CrossRef]
29. Hetta, H.F.; Ramadan, Y.N.; Al-Harbi, A.I.; AAhmed, E.; Battah, B.; Abd Ellah, N.H.; Donadu, M.G. Nanotechnology as a Promising Approach to Combat Multidrug Resistant Bacteria: A Comprehensive Review and Future Perspectives. *Biomedicines* **2023**, *11*, 413. [CrossRef] [PubMed]
30. Buszewski, B.; Railean-Plugaru, V.; Pomastowski, P.; Rafińska, K.; Szultka-Mlynska, M.; Golinska, P.; Wypij, M.; Laskowski, D.; Dahm, H. Antimicrobial activity of biosilver nanoparticles produced by a novel *Streptacidiphilus durhamensis* strain. *J. Microbiol. Immunol. Infect.* **2018**, *51*, 45–54. [CrossRef]
31. Pugazhendhi, A.; Prabakar, D.; Jacob, J.M.; Karuppusamy, I.; Saratale, R.G. Synthesis and characterization of silver nanoparticles using Gelidium amansii and its antimicrobial property against various pathogenic bacteria. *Microb. Pathog.* **2018**, *114*, 41–45. [CrossRef]
32. Tyagi, P.K.; Mishra, R.; Khan, F.; Gupta, D.; Gola, D. Antifungal effects of silver nanoparticles against various plant pathogenic fungi and its safety evaluation on *Drosophila melanogaster*. *Biointerface Res. Appl. Chem.* **2020**, *10*, 6587–6596.
33. El-Nagar, A.; Elzaawely, A.A.; Taha, N.A.; Nehela, Y. The antifungal activity of gallic acid and its derivatives against *Alternaria solani*, the causal agent of tomato early blight. *Agronomy* **2020**, *10*, 1402. [CrossRef]
34. Shinde, B.A.; Dholakia, B.B.; Hussain, K.; Aharoni, A.; Giri, A.P.; Kamble, A.C. WRKY1 acts as a key component improving resistance against *Alternaria solani* in wild tomato, *Solanum arcanum* Peralta. *Plant Biotechnol. J.* **2018**, *16*, 1502–1513. [CrossRef]

35. Panno, S.; Davino, S.; Caruso, A.G.; Bertacca, S.; Crnogorac, A.; Mandić, A.; Noris, E.; Matić, S. A review of the most common and economically important diseases that undermine the cultivation of tomato crop in the mediterranean basin. *Agronomy* **2021**, *11*, 2188. [CrossRef]
36. Ashraf, H.J.; Aguila, L.C.R.; Ahmed, S.; Haq, I.U.; Ali, H.; Ilyas, M.; Gu, S.; Wang, L. Comparative transcriptome analysis of *Tamarixia radiata* (Hymenoptera: Eulophidae) reveals differentially expressed genes upon heat shock. *Comp. Biochem. Physiol.-D Genom. Proteom.* **2022**, *41*, 100940. [CrossRef]
37. El-Ganainy, S.M.; El-Abeid, S.E.; Ahmed, Y.; Iqbal, Z. Morphological and molecular characterization of large-spored I species associated with potato and tomato early blight in Egypt. *Int. J. Agric. Biol.* **2021**, *25*, 1101–1110. [CrossRef]
38. Al-lami, H.F.; You, M.P.; Mohammed, A.E.; Barbetti, M.J. Virulence variability across the *Alternaria spp.* population determines incidence and severity of *Alternaria* leaf spot on rapeseed. *Plant Pathol.* **2020**, *69*, 506–517. [CrossRef]
39. Aslam, M.; Habib, A.; Sahi, S.T.; Khan, R.R. Effect of Bion and Salicylic acid on peroxidase activity and total phenolics in tomato against *Alternaria solani*. *Pak. J. Agric. Sci.* **2020**, *57*, 53–62.
40. Sarfraz, M.; Khan, S.; Moosa, A.; Farzand, A.; Ishaq, U.; Naeem, I.; Khan, W. Promising antifungal potential of selective botanical extracts, fungicides and *Trichoderma* isolates against *Alternaria solani*. *Cercet. Agron. Mold.* **2018**, *51*, 65–74. [CrossRef]
41. Al-Abboud, M.A. Fungal biosynthesis of silver nanoparticles and their role in control of Fusarium wilt of sweet pepper and soil-borne fungi in vitro. *Int. J. Pharmacol.* **2018**, *14*, 773–780. [CrossRef]
42. Domsch, K.H.; Gams, W.; Anderson, T.-H. *Compendium of soil fungi. Volume 1*; Academic Press (London) Ltd.: London, UK, 1980.
43. Ellis, M.B. *Dematiaceous Hyphomycetes*; Commonwealth Mycological Institute: London, UK, 1971.
44. Akhtar, K.P.; Saleem, M.Y.; Asghar, M.; Haq, M.A. New report of Alternaria alternata causing leaf blight of tomato in Pakistan. *Plant Pathol.* **2004**, *53*, 816. [CrossRef]
45. Simmons, E.G. *Alternaria: An Identification Manual*; CBS: New York, NY, USA, 2007.
46. Bruns, T.D.; Gardes, M. Molecular tools for the identification of ectomycorrhizal fungi—Taxon-specific oligonucleotide probes for suilloid fungi. *Mol. Ecol.* **1993**, *2*, 233–242. [CrossRef] [PubMed]
47. White, T.J.; Bruns, T.; Lee, S.; Taylor, J. Amplification and direct sequencing of fungal ribosomal RNA genes for phylogenetics. In *PCR Protocols: A Guide to Methods and Applications*; Innis, M.A., Gelfand, D.H., Sninsky, J.J., White, T.J., Eds.; Academic Press: San Diego, CA, USA, 1990; pp. 315–322.
48. Kim, S.W.; Jung, J.H.; Lamsal, K.; Kim, Y.S.; Min, J.S.; Lee, Y.S. Antifungal effects of silver nanoparticles (AgNPs) against various plant pathogenic fungi. *Mycobiology* **2012**, *40*, 53–58. [CrossRef] [PubMed]
49. Chaerani, C.; Kardin, M.K.; Suhardi, S.; Sofiari, E.; van Ginkel, R.V.; Groenwolt, R.; Voorrips, R.E. Variation in aggressiveness and AFLP among *Alternaria solani* isolates from indonesia. *Indones. J. Agric. Res.* **2017**, *18*, 51–62. [CrossRef]
50. Vakalounakis, D.; DJ, V. *Evaluation of Tomato Cultivars for Resistance to Alternaria Blight*; FAO: Rome, Italy, 1983.
51. Fu, J.; Huang, B. Involvement of antioxidants and lipid peroxidation in the adaptation of two cool-season grasses to localized drought stress. *Environ. Exp. Bot.* **2001**, *45*, 105–114. [CrossRef]
52. Mayer, A.M.; Harel, E.; Ben-Shaul, R. Assay of catechol oxidase—A critical comparison of methods. *Phytochemistry* **1966**, *5*, 783–789. [CrossRef]
53. Burrell, M.M.; Ap Rees, T. Metabolism of phenylalanine and tyrosine by rice leaves infected by Piricularia oryzae. *Physiol. Plant Pathol.* **1974**, *4*, 497–508. [CrossRef]
54. Rana, A.; Yadav, K.; Jagadevan, S. A comprehensive review on green synthesis of nature-inspired metal nanoparticles: Mechanism, application and toxicity. *J. Clean. Prod.* **2020**, *272*, 122880. [CrossRef]
55. Khan, S.; Almarhoon, Z.M.; Bakht, J.; Mabkhot, Y.N.; Rauf, A.; Shad, A.A. Single-Step Acer pentapomicum-Mediated Green Synthesis of Silver Nanoparticles and Their Potential Antimicrobial and Antioxidant Activities. *J. Nanomater.* **2022**, *2022*, 3783420. [CrossRef]
56. Ghazali, S.Z.; Mohamed Noor, N.R.; Mustaffa, K.M.F. Anti-plasmodial activity of aqueous neem leaf extract mediated green synthesis-based silver nitrate nanoparticles. *Prep. Biochem. Biotechnol.* **2022**, *52*, 99–107. [CrossRef]
57. Pawar, A.A.; Sahoo, J.; Verma, A.; Alswieleh, A.M.; Lodh, A.; Raut, R.; Lakkakula, J.; Jeon, B.-H.; Islam, M. Azadirachta indica-Derived Silver Nanoparticle Synthesis and Its Antimicrobial Applications. *J. Nanomater.* **2022**, *2022*, 4251229. [CrossRef]
58. Asif, M.; Yasmin, R.; Asif, R.; Ambreen, A.; Mustafa, M.; Umbreen, S. Green Synthesis of Silver Nanoparticles (AgNPs), Structural Characterization, and their Antibacterial Potential. *Dose-Response* **2022**, *20*, 15593258221088709. [CrossRef]
59. Chakravarty, A.; Ahmad, I.; Singh, P.; Sheikh, M.U.D.; Aalam, G.; Sagadevan, S.; Ikram, S. Green synthesis of silver nanoparticles using fruits extracts of *Syzygium cumini* and their bioactivity. *Chem. Phys. Lett.* **2022**, *795*, 139493. [CrossRef]
60. AlMasoud, N.; Alhaik, H.; Almutairi, M.; Houjak, A.; Hazazi, K.; Alhayek, F.; Aljanoubi, S.; Alkhaibari, A.; Alghamdi, A.; Soliman, D.A. Green nanotechnology synthesized silver nanoparticles: Characterization and testing its antibacterial activity. *Green Process. Synth.* **2021**, *10*, 518–528. [CrossRef]
61. Kumar, S.; Taneja, S.; Banyal, S.; Singhal, M.; Kumar, V.; Sahare, S.; Lee, S.-L.; Choubey, R.K. Bio-synthesised silver nanoparticle-conjugated l-cysteine ceiled Mn: ZnS quantum dots for eco-friendly biosensor and antimicrobial applications. *J. Electron. Mater.* **2021**, *50*, 3986–3995. [CrossRef]
62. Varadavenkatesan, T.; Selvaraj, R.; Vinayagam, R. Dye degradation and antibacterial activity of green synthesized silver nanoparticles using *Ipomoea digitata* Linn. flower extract. *Int J Environ. Sci Technol* **2019**, *16*, 2395–2404. [CrossRef]

63. Zhang, X.-F.; Liu, Z.-G.; Shen, W.; Gurunathan, S. Silver nanoparticles: Synthesis, characterization, properties, applications, and therapeutic approaches. *Int. J. Mol. Sci.* **2016**, *17*, 1534. [CrossRef] [PubMed]
64. Kedi, P.B.E.; Nanga, C.C.; Gbambie, A.P.; Deli, V.; Meva, F.E.; Mohamed, H.E.A.; Ntoumba, A.A.; Nko, M.H.J. Biosynthesis of silver nanoparticles from *Microsorum punctatum* (l.) copel fronds extract and an in-vitro anti-inflammation study. *J. Nanotechnol.* **2020**, *2*, 25–41.
65. Iqbal, S.; Arifeen, S.; Akbar, A.; Zahoor, S.; Maher, S.; Khan, N.; Anwar, H.; Sajjad, A. Phytochemical screening and antibacterial assay of the crude extract and fractions of Ferula oopoda. *Pure Appl. Biol. (PAB)* **2019**, *8*, 742–749. [CrossRef]
66. Abootalebi, S.N.; Mousavi, S.M.; Hashemi, S.A.; Shorafa, E.; Omidifar, N.; Gholami, A. Antibacterial effects of green-synthesized silver nanoparticles using *Ferula asafoetida* against *Acinetobacter baumannii* isolated from the hospital environment and assessment of their cytotoxicity on the human cell lines. *J. Nanomater.* **2021**, *2021*, 6676555. [CrossRef]
67. Niazmand, R.; Razavizadeh, B.M. Active polyethylene films incorporated with β-cyclodextrin/ferula asafoetida extract inclusion complexes: Sustained release of bioactive agents. *Polym. Test.* **2021**, *95*, 107113. [CrossRef]
68. Erenler, R.; Dag, B. Biosynthesis of silver nanoparticles using *Origanum majorana* L. and evaluation of their antioxidant activity. *Inorg. Nano-Met. Chem.* **2022**, *52*, 485–492.
69. Asimuddin, M.; Shaik, M.R.; Adil, S.F.; Siddiqui, M.R.H.; Alwarthan, A.; Jamil, K.; Khan, M. Azadirachta indica based biosynthesis of silver nanoparticles and evaluation of their antibacterial and cytotoxic effects. *J. King Saud Univ. Sci.* **2020**, *32*, 648–656. [CrossRef]
70. Aziz, S.; Hussein, G.; Brza, M.J.; Mohammed, S.T. Abdulwahid, R.; Raza Saeed, S.; Hassanzadeh, A. Fabrication of interconnected plasmonic spherical silver nanoparticles with enhanced localized surface plasmon resonance (LSPR) peaks using quince leaf extract solution. *Nanomaterials* **2019**, *9*, 1557. [CrossRef] [PubMed]
71. Mohamed, Y.M.A.; Elshahawy, I.E. Antifungal activity of photo-biosynthesized silver nanoparticles (AgNPs) from organic constituents in orange peel extract against phytopathogenic Macrophomina phaseolina. *Eur. J. Plant Pathol.* **2022**, *162*, 725–738. [CrossRef]
72. Iravani, S.; Varma, R.S. Biofactories: Engineered nanoparticles via genetically engineered organisms. *Green Chem.* **2019**, *21*, 4583–4603. [CrossRef]
73. Chen, L.; Zhou, X.; Shi, Y.; Gao, B.; Wu, J.; Kirk, T.B.; Xu, J.; Xue, W. Green synthesis of lignin nanoparticle in aqueous hydrotropic solution toward broadening the window for its processing and application. *J. Chem. Eng.* **2018**, *346*, 217–225. [CrossRef]
74. Riaz, H.; Chohan, S.; Abid, M. Occurrence of tomato early blight disease and associated *Alternaria* species in Punjab, Pakistan. *J Anim Plant Sci* **2021**, *31*, 1352–1365.
75. Akhtar, K.P.; Ullah, N.; Saleem, M.Y.; Iqbal, Q.; Asghar, M.; Khan, A.R. Evaluation of tomato genotypes for early blight disease resistance caused by *Alternaria solani* in Pakistan. *J. Plant Pathol.* **2019**, *101*, 1159–1170. [CrossRef]
76. Ayad, D.; Aribi, D.; Hamon, B.; Kedad, A.; Simoneau, P.; Bouznad, Z. Distribution of large-spored *Alternaria* species associated with early blight of potato and tomato in Algeria. *Phytopathol. Mediterr.* **2019**, *58*, 139–149.
77. Hussain, A.; Ali, S.; Abbas, H.; Ali, H.; Hussain, A.; Khan, S.W. Spatial distribution of early blight disease on tomato, climatic factors and bio efficacy of plant extracts against *Alternaria solani*. *Acta Sci. Pol. Hortorum Cultus* **2019**, *18*, 29–38. [CrossRef]
78. Pahnwar, S.; Khaskheli, M.; Khaskheli, A.; Wagan, K. Isolation and Identification of Different Fungal Species from Major Kharif Vegetables of Sindh Province, Pakistan. *Agric. Sci. Dig.* **2021**, *1*, 1–6. [CrossRef]
79. Ding, S.; Meinholz, K.; Cleveland, K.; Jordan, S.A.; Gevens, A.J. Diversity and virulence of *Alternaria spp.* causing potato early blight and brown spot in Wisconsin. *Phytopathology* **2019**, *109*, 436–445. [CrossRef] [PubMed]
80. Belosokhov, A.; Belov, G.; Chudinova, E.; Kokaeva, L.Y.; Elansky, S. *Alternaria* spp. and *Colletotrichum coccodes* in potato leaves with early blight symptoms. *PAGV–Spec. Rep.* **2017**, *18*, 181–190.
81. Ramezani, Y.; Taheri, P.; Mamarabadi, M. Identification of *Alternaria* spp. associated with tomato early blight in Iran and investigating some of their virulence factors. *J. Plant Pathol.* **2019**, *101*, 647–659. [CrossRef]
82. Özer, N.; Kün, A.; İlbi, H. Detached leaf test for evaluation of resistance to powdery mildew in pepper. *J. Agric. Sci. Technol.* **2018**, *14*. [CrossRef]
83. Meena, M.; Swapnil, P.; Zehra, A.; Dubey, M.K.; Upadhyay, R. Antagonistic assessment of *Trichoderma spp.* by producing volatile and non-volatile compounds against different fungal pathogens. *Arch. Phytopathol. Pflanzenschutz* **2017**, *50*, 629–648. [CrossRef]
84. Al-Otibi, F.; Alfuzan, S.A.; Alharbi, R.I.; Al-Askar, A.A.; Al-Otaibi, R.M.; Al Subaie, H.F.; Moubayed, N.M. Comparative study of antifungal activity of two preparations of green silver nanoparticles from Portulaca oleracea extract. *Saudi J. Biol. Sci.* **2022**, *29*, 2772–2781. [CrossRef]
85. Rizwana, H.; Alwhibi, M.S.; Aldarsone, H.A.; Awad, M.A.; Soliman, D.A.; Bhat, R.S. Green synthesis, characterization, and antimicrobial activity of silver nanoparticles prepared using *Trigonella foenum*-graecum L. leaves grown in Saudi Arabia. *Green Process. Synth.* **2021**, *10*, 421–429. [CrossRef]
86. Guilger-Casagrande, M.; Lima, R.d. Synthesis of silver nanoparticles mediated by fungi: A review. *Front. Bioeng. Biotechnol.* **2019**, *7*, 287. [CrossRef]
87. Mostafa, Y.S.; Alamri, S.A.; Alrumman, S.A.; Hashem, M.; Baka, Z.A. Green Synthesis of Silver Nanoparticles Using Pomegranate and Orange Peel Extracts and Their Antifungal Activity against *Alternaria solani*, the Causal Agent of Early Blight Disease of Tomato. *Plants* **2021**, *10*, 2363. [CrossRef] [PubMed]

88. Yan, X.; He, B.; Liu, L.; Qu, G.; Shi, J.; Hu, L.; Jiang, G. Antibacterial mechanism of silver nanoparticles in *Pseudomonas aeruginosa*: Proteomics approach. *Metallomics* **2018**, *10*, 557–564. [CrossRef] [PubMed]
89. Kumari, M.; Pandey, S.; Giri, V.P.; Bhattacharya, A.; Shukla, R.; Mishra, A.; Nautiyal, C. Tailoring shape and size of biogenic silver nanoparticles to enhance antimicrobial efficacy against MDR bacteria. *Microb. Pathog.* **2017**, *105*, 346–355. [CrossRef] [PubMed]
90. Ashraf, H.; Anjum, T.; Riaz, S.; Naseem, S. Microwave-assisted green synthesis and characterization of silver nanoparticles using Melia azedarach for the management of Fusarium wilt in tomato. *Front. Microbiol.* **2020**, *11*, 238. [CrossRef] [PubMed]
91. Kumari, M.; Pandey, S.; Bhattacharya, A.; Mishra, A.; Nautiyal, C.S. Protective role of biosynthesized silver nanoparticles against early blight disease in *Solanum lycopersicum*. *Plant Physiol. Biochem.* **2017**, *121*, 216–225. [CrossRef]